J Appl Physiol 134: 1520–1529, 2023.
First published May 11, 2023; doi:10.1152/japplphysiol.00080.2023

american physiological society | JOURNAL OF APPLIED PHYSIOLOGY

RESEARCH ARTICLE

Influence of internal muscle properties on muscle shape change and gearing in the human gastrocnemii

Nicole Y. Kelp,[1] Christofer J. Clemente,[1,2] Kylie Tucker,[1] François Hug,[1,3] Sabrina Pinel,[1] and Taylor J. M. Dick[1]

[1]*School of Biomedical Sciences, The University of Queensland, Saint Lucia, Queensland, Australia;* [2]*School of Engineering and Science, University of the Sunshine Coast, Sippy Downs, Queensland, Australia; and* [3]*LAMHESS, Université Côte d'Azur, Nice, France*

Abstract

Skeletal muscles bulge when they contract. These three-dimensional shape changes, coupled with fiber rotation, influence a muscle's mechanical performance by uncoupling fiber velocity from muscle belly velocity (i.e., gearing). Muscle shape change and gearing are likely mediated by the interaction between internal muscle properties and contractile forces. Muscles with greater stiffness and intermuscular fat, due to aging or disuse, may limit a muscle's ability to bulge in width, subsequently causing higher gearing. The aim of this study was to determine the influence of internal muscle properties on shape change, fiber rotation, and gearing in the medial (MG) and lateral gastrocnemii (LG) during isometric plantar flexion contractions. Multimodal imaging techniques were used to measure muscle shear modulus, intramuscular fat, and fat-corrected physiological cross-sectional area (PCSA) at rest, as well as synchronous muscle architecture changes during submaximal and maximal contractions in the MG and LG of 20 young (24 ± 3 yr) and 13 older (70 ± 4 yr) participants. Fat-corrected PCSA was positively associated with fiber rotation, gearing, and changes in thickness during submaximal contractions, but it was negatively associated with changes in thickness at maximal contractions. Muscle stiffness and intramuscular fat were related to muscle bulging and reduced fiber rotation, respectively, but only at high forces. Furthermore, the MG and LG had varied internal muscle properties, which may relate to the differing shape changes, fiber rotations, and gearing behaviors observed at each contraction level. These results indicate that internal muscle properties may play an important role in mediating in vivo muscle shape change and gearing, especially during high-force contractions.

NEW & NOTEWORTHY Here, we measured internal muscle properties in vivo to determine their influence on the varying shape change and gearing behaviors in the synergistic gastrocnemii muscles. These relationships have previously only been hypothesized or examined within isolated muscles during supramaximal contractions. Our results contribute to a more comprehensive understanding of the factors that influence a muscle's mechanical response to force with implications for preventing or treating muscle deficits associated with aging, disease, and disuse.

aging; intramuscular fat; physiological cross-sectional area; stiffness; ultrasound

INTRODUCTION

When skeletal muscle contracts, fibers shorten and rotate to steeper pennation angles. Due to the nearly isovolumetric nature of muscles (1), these changes in length are accompanied by changes in muscle thickness and/or width. The direction in which a muscle changes shape (i.e., thickness or width) and the extent to which muscle fibers rotate during a contraction influence its mechanical performance—enabling the muscle fibers to shorten at different (typically more optimal) velocities than that of the whole muscle, a process known as gearing (2, 3). Low-force high-velocity contractions are associated with high gearing, due to large fiber rotations and increased thickness, whereas high-force low-velocity contractions are associated with low gearing, less fiber rotation, and smaller changes in thickness (2, 4–6). Declines in muscle performance associated with aging and disease may be linked to alterations in a muscle's ability to change shape and gear (4, 7). However, the mechanisms underpinning in vivo shape changes and gearing in both young and aging muscles are not fully understood.

We have previously shown that the relationship between changes in pennation angle and muscle thickness varies in the human medial gastrocnemius (MG) and lateral gastrocnemius (LG; 8), suggesting that the architectural and mechanical properties of individual muscles, herein referred to as internal muscle properties, may play a role. Muscle shape change and gearing are governed by the interaction between the forces produced by the contractile elements (muscle fibers) and the resistance to these forces owing to internal

Correspondence: N. Y. Kelp (n.kelp@uq.edu.au).
Submitted 9 February 2023 / Revised 2 May 2023 / Accepted 3 May 2023

8750-7587/23 Copyright © 2023 the American Physiological Society.

Downloaded from journals.physiology.org/journal/jappl (078.056.041.167) on November 9, 2026.

muscle properties such as connective tissues and fluid pressure (4, 9–12). Intramuscular connective tissue surrounds the whole muscle, comprising the superficial and deep aponeurosis, with other layers surrounding individual muscle fibers, as well as muscle fiber bundles (fascicles). It is hypothesized that, as muscle fibers shorten, they produce a force that acts to pull the aponeuroses together and decrease muscle thickness, whereas the connective tissues within and surrounding the muscle fibers resist the muscle from bulging in width (4, 11, 12). There is growing evidence that this interplay, between the contractile forces and connective tissue resistance, plays an important role in modulating shape change and gearing. For example, Holt et al. (4) demonstrated that stiffer muscles in older rats had a reduced ability to vary gearing, and thereby operated at high gearing through a range of contractile conditions. Although this study did not directly measure changes in pennation angle and thickness, they attributed this loss of variable gearing to the muscle's inability to transition from bulging in thickness at low forces, to bulging in width during high-force contractions. Eng et al. (11) showed that altering the connective tissue properties via longitudinal aponeurosis incisions leads to lower gearing during high-force, but not during low-force, contractions. Together, these studies highlight that connective tissue properties influence a muscle's mechanical output via altering shape changes and gearing during high-force contractions.

Another factor that may affect a muscle's shape change and gearing capacity is intramuscular fat. The infiltration of fat into skeletal muscle reduces the proportion of contractile tissue and leads to a reduction in maximum isometric stress (13). Greater intramuscular fat is associated with aging (14), inactivity (15), and disease (16). Previous modeling studies have shown that introducing fat into a muscle lead to lower specific forces and an overall increase in the stiffness of the muscle (17). The infiltration of fat into skeletal muscle may act to resist radial fiber expansion and therefore fiber shortening. However, we have previously found that higher proportions of intramuscular fat in the human gastrocnemii are associated with lower shear modulus values (14). Thus, we still have a limited understanding of how intramuscular fat influences in vivo muscle shape change and gearing.

The magnitude of contractile forces a muscle can generate is determined by the number and arrangement of fibers within a muscle. Physiological cross-sectional area (PCSA) provides an estimate of a muscle's maximum force-generating capacity (18) and can be calculated as the ratio of muscle volume to fiber length (19). This force estimate can be further improved by correcting the muscle volume for the amount of intramuscular fat, thereby only including the contractile component of the muscle volume (i.e., fat-corrected PCSA). PCSA may affect how muscles change shape and gear as muscles with greater PCSA have more fibers arranged in parallel, providing a greater force that tends to pull the aponeuroses together and decrease the muscle thickness. The medial gastrocnemius has greater fat-corrected PCSA compared with the lateral gastrocnemius, owing to its greater volume and shorter more pennate fascicles (14). Previous experimental studies have shown that the MG undergoes smaller changes in thickness at high contraction levels (8, 20). Brainerd and Azizi (3) used a segmented muscle model to demonstrate that within a single muscle, fibers with greater pennation angles operated at higher gearing. These studies suggest that variation in muscle architecture, both within and between muscles, influences mechanical behavior. Although much of our knowledge about the mechanisms that underpin shape changes and gearing has come from elegant experiments conducted under controlled conditions, these studies may overlook the important phenomena of muscle behavior that occur in vivo. The interplay between architectural and mechanical muscle properties, herein referred to as internal muscle properties (i.e., connective tissue stiffness, intramuscular fat, and PCSA), may constrain how a muscle changes shape and gears during varying contractions (11, 12)—with likely implications for locomotor performance.

In this study, we used multimodal imaging techniques including T1 and mDIXON magnetic resonance imaging (MRI), shear wave elastography (SWE), and B-mode ultrasound to explore the influence of internal muscle properties on in vivo muscle shape changes and gearing in the gastrocnemii of young and older adults. We included both the MG and LG and young and older adults in this study, given the previously identified differences in internal muscle properties between these muscles and populations (14). Specifically, we aimed to determine the influence of muscle shear modulus (an index of stiffness), intramuscular fat, and fat-corrected PCSA on muscle shape change, pennation angle, and gearing during submaximal and maximal isometric plantarflexion contractions. We hypothesize that greater muscle shear modulus and intramuscular fat will be associated with increased thickness and pennation angle and higher gearing across all contraction levels, based on previous findings that greater muscle stiffness leads to higher gearing in aging rats (4) and that intramuscular fat may restrict fiber shortening due to increased overall muscle stiffness (17). We also hypothesize that greater fat-corrected PCSA will be associated with higher pennation angles and gearing; however, these changes may not be associated with increased thickness due to muscles with greater PCSA typically having greater resting pennation angle (14) and more fibers in parallel, thus producing a greater force that compresses the muscle in the thickness direction.

MATERIALS AND METHODS

Data were collected from 20 young (24 ± 2.5 yr, 8 women) and 13 older (70 ± 4.2 yr, 5 women) participants across two sessions: an MRI session and a laboratory session. All participants met the minimum physical activity requirements as per Active Australia Self-Report Physical Activity Measure [>600 metabolic equivalent of task (MET) min/wk] and an MRI-safe checklist (i.e., no pacemaker or metal implants). Exclusion criteria included lower limb pain or injury in the past 6 mo. Before collection, participants gave written informed consent, and all experimental protocols were approved by The University of Queensland's Human Research Ethics Committee (No. 2013001448).

The MRI session consisted of two scanning sequences of the triceps surae: *1*) a T1-weighted scan to determine muscle volume (Fig. 1, *D* and *E*) and *2*) an mDIXON scan to determine intramuscular fat (Fig. 1*F*). During the laboratory

Downloaded from journals.physiology.org/journal/jappl (078.056.041.167) on November 9, 2026.

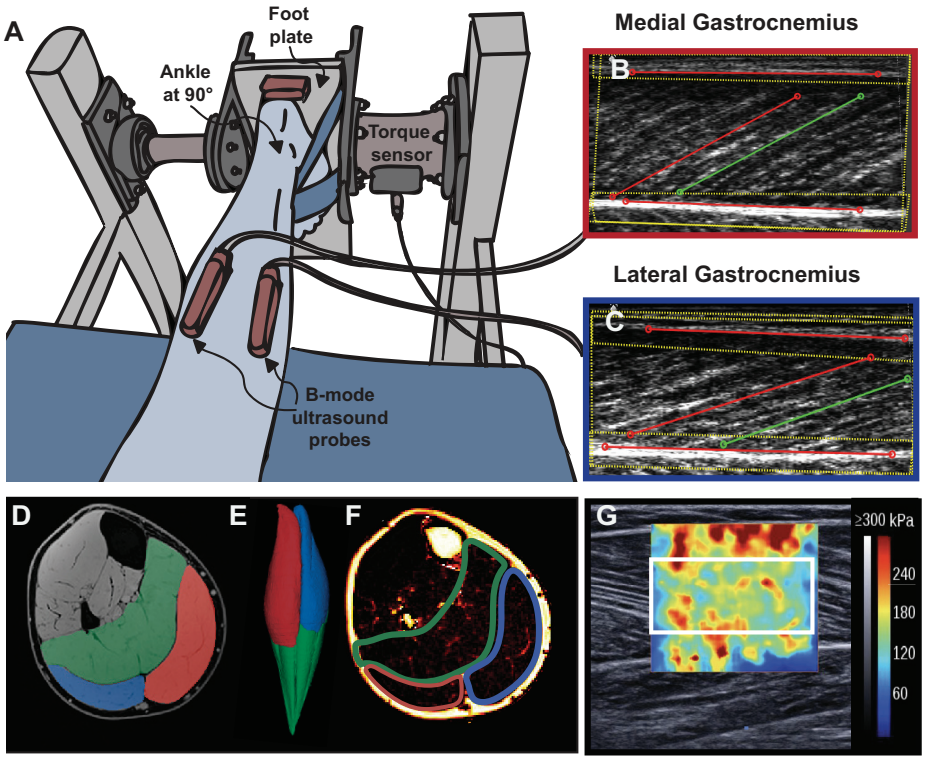


Figure 1. *A*: experimental setup of isometric plantar flexion contractions whereby a dual-probe ultrasound configuration was used to synchronously image the medial gastrocnemius (MG; *B*) and lateral gastrocnemius (LG; *C*). *D*: example of a T1-weighted MRI slice with segmented MG (red), LG (blue), and soleus (SOL; green), a full three-dimensional reconstruction of the triceps surae (posterior view; *E*), and the intramuscular fat maps obtained from the mDIXON scans (*F*). *G*: muscle shear modulus was measured during passive dorsiflexion using shear wave elastography shown for the MG, with the scale for Young's modulus displayed on the right. Warmer colors indicate "stiffer," whereas cool colors indicate "less stiffness."

session, we first quantified medial gastrocnemius (MG), lateral gastrocnemius (LG), and soleus (SOL) muscle shear modulus using SWE (Fig. 1*G*) and resting muscle architecture (fascicle length, pennation angle, and thickness) using B-mode ultrasound. Following this, the participants conducted a series of submaximal and maximal isometric plantarflexion contractions while we measured dynamic changes in muscle architecture and shape simultaneously in the MG and LG (Fig. 1, *B* and *C*) using a dual-probe ultrasound configuration (Fig. 1*A*).

Intramuscular Fat

Muscle volume was determined from the T1-weighted scans. An experienced examiner used both semiautomated (Sashimi Segmentation V1.1; Bolsterlee 2020) and manual approaches (ITK-SNAP v3.8.0, NIH) to segment the MG, LG, and SOL on all image slices the muscle was visible (Fig. 1*D*), creating a three-dimensional (3-D) reconstruction of the muscle volume (Fig. 1*E*). To determine the percentage of intramuscular fat within the individual muscles, the T1-weighted segmentations were overlaid with a fat fraction map obtained from the mDIXON scans (Fig. 1*F*). The mDIXON scans provide separate fat-saturated and water-saturated images, produced by using an in-phase and out-of-phase image that captures the chemical shift difference between water and fat (21). Further details regarding the data collection and analysis of the MRI scans and calculations of fat fractions can be found in the study by Pinel et al. (14). To calculate the fat-corrected muscle volume for the MG, LG, and SOL, the percentage volume of intramuscular fat was subtracted from the total muscle volume.

Fat-Corrected PCSA

To determine the fat-corrected PCSA, we divided fat-corrected muscle volume, from the mDIXON MRI scans, by resting fascicle length, determined from the B-mode ultrasound (details as follows):

$$\text{Fat-corrected PCSA} = \frac{\text{Fat-corrected muscle volume}}{\text{Fascicle length}} \quad (1)$$

Resting Muscle Architecture

Resting fascicle length, pennation angle, and thickness of the MG, LG, and SOL were measured in a relaxed state using B-mode ultrasound (version 9.3; SuperSonic Imagine, Aix-en-Provence, France) with a linear transducer (56 mm, 4–15 MHz, VERMON, Tours, France). Participants laid prone with their knee extended and ankle at 90° against a stationary foot plate (Fig. 1*A*). For the MG and LG, two images were acquired at both the middle proximal and the middle distal regions of the muscle belly. For the SOL, the images were acquired on both lateral and medial distal regions. Ultrasound images were analyzed with a custom ImageJ Plug-in Macro (v1.52, National Institutes of Health, Bethesda, MD). Resting values for fascicle length, pennation angle, and muscle thickness of the MG, LG, and SOL were calculated as the average of the four images (i.e., both images taken at each region).

Shear Wave Elastography

Shear wave elastography was used to determine muscle shear modulus (kPa; 22) during passive dorsiflexion (23). Shear wave elastography relies on the measurement of shear

Downloaded from journals.physiology.org/journal/jappl (078.056.041.167) on November 9, 2026.

wave velocity that results from mechanical perturbations to the tissue. Shear modulus (μ) is related to the shear wave velocity (V_s):

$$\mu = \rho V_s^2 \quad (2)$$

where ρ is the density of the tissue (1,000 kg/m^3 for muscle), such that the stiffer the tissue the faster the shear wave propagation. SWE has been validated against traditional material testing to provide an estimate of muscle stiffness (24). A full description regarding the collection and analysis of muscle shear modulus can be found in the study by Pinel et al. (14). In brief, in this study, shear modulus of the MG and LG was determined $+5^\circ$ from fascicle slack length, as an indication of stiffness within the muscle at a normalized length. SWE measurements in the SOL were excluded from analysis due to poor image quality, along with the MG of three participants and LG of two participants.

Isometric Plantarflexion Contractions

Participants performed a series of isometric plantarflexion contractions while lying prone with their knee fully extended and ankle at 90° on a fixed ankle dynamometer (Model TRE-50K, Dacell co., ltd, Chungbuk, Republic of Korea) (Fig. 1*A*). Positive (plantar flexion) and negative (dorsiflexion) torque signals from the dynamometer were sent through a data acquisition board (CED 1401, Cambridge Electronic Design Ltd., Milton, Cambridge, England) and recorded in Spike2 software (v7.17, Cambridge Electronic Design Ltd., Milton, Cambridge, England). Participants were verbally encouraged to perform maximum isometric plantar flexion contractions by pushing through the ball of their foot and engaging their calf muscles while maintaining heel contact on the footplate. Maximal voluntary contractions (MVCs) were performed at minimum three times until the maximum plantarflexion torque was within 10% of the previous trial with 2-min rest between each MVC trial. The highest plantarflexion torque achieved was used to calculate submaximal torque levels representing 10%, 30%, and 50% of MVC. Feedback of the torque signal was provided to the participant on a screen, in addition to a target line (at each submaximal torque level, respectively). Submaximal contractions were repeated for three trials in random order with an equal percent to seconds rest between each trial (e.g., 30-s rest at the 30% contraction level).

B-Mode Ultrasound

Two B-mode ultrasound devices (ArtUs EXT-1H, REV: C1S, Telemed, Vilnius, Lithuania) were used to simultaneously image the MG and LG during the submaximal and maximal isometric plantar flexion contractions. The linear ultrasound probes (LV8-5L60N-2, 60 mm, 5–8 MHz, Telemed, Vilnius, Lithuania) were placed over each midregion of the muscle belly and aligned with the fascicle plane. Images were recorded using Echo Wave II software (Telemed, Vilnius, Lithuania) at ~135 Hz. The trigger signal from each ultrasound scanner was recorded in Spike2 to synchronize with the torque signal from the dynamometer.

Semiautomated ultrasound tracking software (UltraTrack v5.3) was used to determine the time-varying fascicle length, pennation angle, and muscle thickness of the MG and LG during the isometric contractions. This version was adapted by Doguet and Hauraix (v.5.3, 2019) from the original UltraTrack (Lichtwarck and Farris, v4.2, 2016). The tracking algorithm uses an affine optic flow (25) to track tissues in subsequent frames of the video. Regions of interest (ROI) and tissues were manually identified around the superficial and deep aponeurosis and whole muscle and two fascicles were tracked within each frame (Fig. 1, *B* and *C*). Tracking data were exported for further processing (v11.3, Wolfram Research, Inc., Champaign, IL). Ultrasound data were synchronized with the torque signals from the onset of torque rise to the first point at which target torque was reached. Projected muscle belly length (L_b) was calculated as fascicle length multiplied by cosine pennation angle (β):

$$L_b = L_f \times \mathrm{Cos}\beta \quad (3)$$

Fascicle length and belly length data were low-pass filtered at 12 Hz. Fascicle velocity and muscle belly velocity were calculated as the first-time derivatives of the changes in fascicle length and belly length, respectively. Gearing was calculated as the ratio of muscle belly velocity to fascicle velocity at the point of maximum belly shortening velocity (6). Changes in fascicle length and muscle thickness were normalized to resting fascicle length and muscle thickness, whereas changes in pennation angle are expressed in degrees.

Statistical Analysis

Statistical analysis was performed in R (v3.4.3, Vienna, Austria). Differences in participant characteristics (age, maximum ankle plantar flexion torque, body mass, height, and METmin physical activity) were assessed using Welch's *t* test. Linear mixed-effects (LME) models (lme.R function from the nlme package; 26) were used to determine the *1*) influence of age and muscle (fixed factors) on muscle volume, pennation angle, muscle thickness, shear modulus, intramuscular fat, and fat-corrected PCSA (as dependent variables); *2*) influence of age, muscle, and condition (fixed factors) on the change in pennation angle, change in thickness, and gearing; and *3*) influence of shear modulus, intramuscular fat, and fat-corrected PCSA on the change in pennation angle, change in thickness, and gearing. In all models, subject was specified as a random factor and a full interaction model was constructed and then reduced to the minimum basic model using backward stepwise regression if interactions were not significant, except for models that explored the relationship between internal muscle properties and muscle shape change and gearing, in which case a full additive model was constructed. Tukey's post hoc tests were then performed using the glht.R function from the multcomp package (27). For all tests, the significance threshold was set to $P = 0.05$. All statistical results regarding the full linear mixed-effects models and Tukey's post hoc tests can be found in the Supplemental Tables S1 and S2 (all Supplemental Material is available at http://doi.org/10.6084/m9.figshare.22059575).

RESULTS

Participant and Muscle Characteristics

Older adults had significantly higher body mass index (BMI; $P = 0.039$), lower ankle plantar flexion torque ($P <$

Downloaded from journals.physiology.org/journal/jappl (078.056.041.167) on November 9, 2026.

Table 1. *Participant characteristics*

	Age, yr	Body Mass, kg	BMI, kg/m^2	Plantar Flexion MVC, N	Physical Activity, MET min/wk
Young, n = 20	24 ± 2.5	71 ± 14.6	24 ± 3.5	128 ± 35.8	556 ± 310.6
Older, n = 13	70 ± 4.2	73 ± 17.8	25 ± 4.7	87 ± 38.2	336 ± 183.2
P value	<0.001*	0.415	0.039*	<0.001*	<0.001*

Values are reported as means ± SD. BMI, body mass index; MVC, maximal voluntary contraction. *Significance level set to $P < 0.05$.

0.001), and were less physically active ($P < 0.001$) compared with young adults (Table 1). There were no differences in resting fascicle length, pennation angle, muscle thickness, or muscle volume (all $P > 0.05$) between young and older adults. However, differences between muscles were observed with the SOL having the greatest muscle volume followed by the MG and LG (all $P < 0.001$). The MG was more pennate and thicker than both the SOL and LG (all $P < 0.001$), whereas the LG had the longest fascicles, followed by the MG then SOL (all $P < 0.001$; Table 2).

Internal Muscle Properties

Shear modulus was not significantly different between young and older adults, however, the MG had greater shear modulus than the LG ($P < 0.001$). Intramuscular fat was greater in older adults compared with young adults across all muscles ($P < 0.001$). There was no difference in intramuscular fat between muscles for young adults, but there was greater intramuscular fat in the MG compared with the LG ($P > 0.001$) for older adults. Differences in fat-corrected PCSA between young and older adults varied depending on the muscle. Older adults had lower fat-corrected PCSA in the MG ($P = 0.034$), but similar fat-corrected PCSA in the LG and SOL as compared with young adults. Across both age groups, the MG had greater fat-corrected PCSA than the LG ($P < 0.001$; Table 3).

Shape Changes and Gearing

Changes in pennation angle and muscle thickness.

Detailed statistics and results can be found in Supplemental Table S1. In brief, changes in pennation angle differed between the MG and LG across contraction levels, and differed between young and older adults, with the MG and young adults demonstrating greater changes in pennation angle with increasing contraction level, compared with the LG and older adults, respectively (all $P < 0.001$). Older adults had smaller changes in muscle thickness compared with young adults regardless of the muscle ($P = 0.028$). The MG and LG also behaved differently at each contraction level. At low contraction levels, such as 10% and 30% MVC, the LG got thinner, whereas the MG had small increases in thickness (both $P < 0.001$). At 50% MVC, the MG and LG had similar increases in thickness but diverged again at 100% MVC with the LG having significantly greater increases in thickness than the MG ($P < 0.001$; Fig. 2).

Gearing.

Gearing increased with contraction level, regardless of age or muscle ($P < 0.001$); however, it was greater in the MG compared with the LG ($P < 0.001$). Older adults operated at lower gearing compared with young adults, independent of contraction level or muscle ($P = 0.030$; Fig. 2).

Influence of Internal Muscle Properties on Muscle Shape Change and Gearing

To determine the influence of internal muscle properties on changes in pennation angle, thickness, and gearing, we did not include muscle and age as factors within our model, as to increase the variability of muscle properties within our dataset. We compared the maximal (100%) and one submaximal contraction level (30% MVC) as this represents the approximate maximal level of muscle activity in the gastrocnemii during level walking (28).

Maximal contractions.

During maximal contractions, shear modulus had a significant negative relationship with changes in muscle thickness ($P = 0.008$), indicating that the stiffer the muscle the less it bulged in thickness. Intramuscular fat had a significant negative relationship with changes in pennation angle ($P = 0.014$), such that muscles with higher fat displayed less fiber

Table 2. *Resting muscle characteristics*

	Muscle Volume, cm^3	Pennation Angle, deg.	Muscle Thickness, mm	Fascicle Length, mm
Young				
LG	150.9 ± 45.6	14.8 ± 3.8	13.3 ± 2.5	56.1 ± 6.3*‡
MG	244.5 ± 65.7*	20.5 ± 3.2*	16.5 ± 2.4*†	51.5 ± 6.8†
SOL	405.7 ± 146.1†‡	20.0 ± 2.5‡	12.5 ± 2.4	36.7 ± 8.4
Older				
LG	138.5 ± 38.0	13.1 ± 2.4	12.5 ± 2.6	58.9 ± 7.3*‡
MG	214.5 ± 62.4*	17.6 ± 3.1*	14.5 ± 2.5†	51.6 ± 6.8†
SOL	433.2 ± 106.1†‡	20.9 ± 4.7†‡	12.3 ± 2.8	33.1 ± 7.8

Values are reported as means ± SD. P values and F statistics can be found in Supplemental Table S1. Significance level set to $P < 0.05$, with symbols indicating difference between *MG and LG; †MG and SOL; ‡LG and SOL. LG, lateral gastrocnemius; MG, medial gastrocnemius; SOL, soleus.

Table 3. *Internal muscle properties*

	Shear Modulus, kPa	Intramuscular Fat, % of Volume	Fat-Corrected PCSA, cm^2
Young			
LG	6.3 ± 2.6	7.1 ± 1.3	25.1 ± 7.2
MG	8.2 ± 2.7*	7.2 ± 1.7	44.4 ± 11.3§*
SOL		7.5 ± 2.3	101.9 ± 26.5†‡
Older			
LG	5.6 ± 1.8	10.5 ± 3.2§	21.1 ± 5.4
MG	9.2 ± 4.0*	12.9 ± 3.9§*	36.3 ± 10.1*
SOL		12.3 ± 2.7§‡	118.2 ± 29.5†‡

Values are reported as means ± SD. P values and F statistics can be found in Supplemental Table S1. Significance level set to $P < 0.05$ with symbols indicating differences between *MG and LG; †MG and SOL; ‡LG and SOL; §young and older adults. LG, lateral gastrocnemius; MG, medial gastrocnemius; PCSA, physiological cross-sectional area; SOL, soleus.

Downloaded from journals.physiology.org/journal/jappl (078.056.041.167) on November 9, 2026.

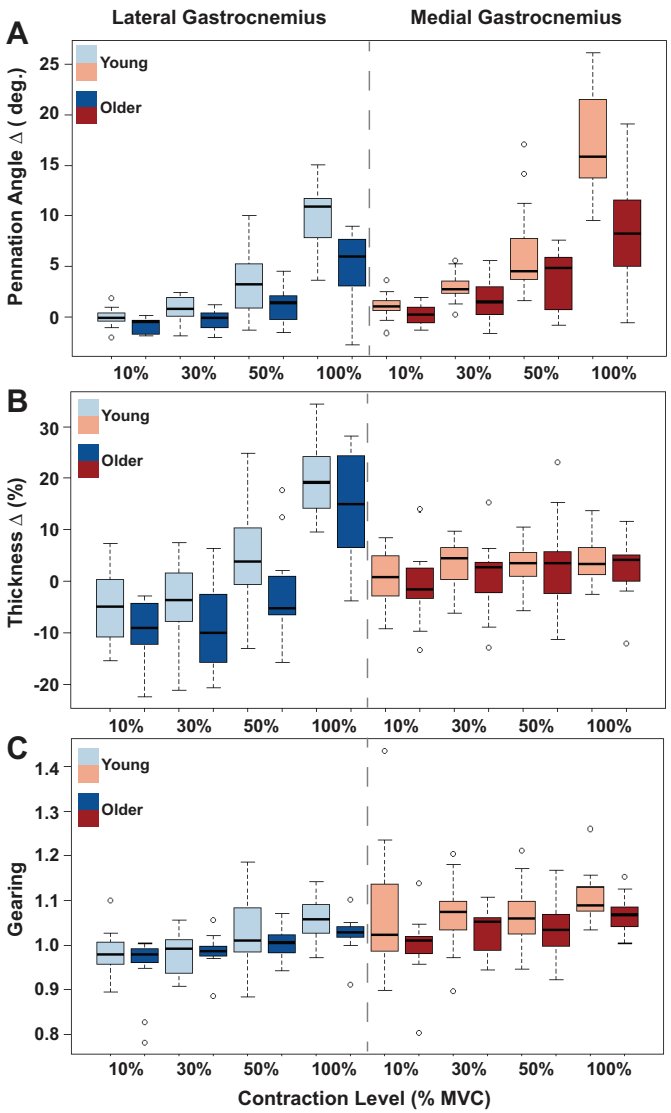


Figure 2. Box and whisker plots for change in pennation angle (deg.; *A*), change in muscle thickness (normalized to resting whereby negative values indicate decreased muscle thickness; *B*), and gearing (*C*). Data are shown for the lateral gastrocnemius (*left*, blue) and the medial gastrocnemius (*right*, red) with the young adults shown in darker colors and older adults shown in lighter colors and box and whisker plots show the median (black line) with hinges representing the first and third quartiles. Whiskers represent the 95% CIs and open circles represent outliers. deg., Degree.

rotation compared with those with lower levels of intramuscular fat. Fat-corrected PCSA had a significant relationship with change in pennation angle, muscle thickness, and gearing (all $P < 0.001$). This meant that muscles with greater fat-corrected PCSA rotated to steeper pennation angles, underwent smaller changes in muscle thickness (even getting thinner at the highest PCSAs), and operated at higher gearing.

Submaximal contractions.

At submaximal contraction levels (30% MVC), shear modulus and intramuscular fat did not influence changes in pennation angle, thickness, or gearing. Similar to maximal contraction levels, the greater the fat-corrected PCSA the more the fibers rotated and the higher the gearing (both $P <$ 0.001). However, during submaximal contractions, greater fat-corrected PCSA was associated with increases in muscle thickness ($P < 0.001$), as opposed to the decreased changes observed at 100% MVC.

DISCUSSION

In this study, we aimed to determine the relationship between internal muscle properties and in vivo muscle shape change and gearing in the human gastrocnemii during isometric plantar flexion contractions. Dynamic changes in muscle shape and gearing enable skeletal muscle to partially circumvent its force-velocity constraints and thus broaden its functional capacity across a range of mechanical demands. We used muscle- and age-related differences in stiffness, intramuscular fat, and architecture to explore the potential influence of these internal muscle properties on shape changes and gearing. The differences in these internal properties between muscles, and in some cases, between young and older adults, demonstrate the suitability of this experimental paradigm to explore our primary aim. We found that in both the medial and lateral gastrocnemii, fibers rotate more and gearing increases with increasing contraction level. However, the MG and LG demonstrated different changes in muscle shape, with the MG having minimal bulging in thickness, whereas the LG bulged substantially in thickness with increasing contraction level, consistent with previous studies (8, 20, 29, 30). Our results show that during high-force contractions, stiffer muscles bulge less in thickness, muscles with higher amounts of intramuscular fat undergo less fiber rotation, and muscles with greater fat-corrected PCSA operate at higher gearing. Interestingly, at submaximal contraction levels, differences in internal muscle properties had a minimal influence on shape changes and gearing.

Previous studies have suggested an intimate link between muscle bulging and gearing. For example, Fig. 2 in Eng et al. (11) demonstrates that low gearing is associated with less fiber rotation and decreased muscle thickness, whereas high gearing is associated with increased fiber rotation and increased or constant muscle thickness. In this study, we found that both fiber rotation and gearing increased with contraction level in the MG and LG, however, changes in muscle thickness were not consistent between the muscles. The MG showed slight increases in thickness, whereas the LG bulged in thickness at maximal contraction levels. The increases in pennation angle with contraction level demonstrated here are consistent with previous studies (8, 20, 29, 31). However, increases in gearing with increasing force are inconsistent with previous studies that have measured gearing during isotonic fixed-end contractions (2, 4, 32). These differences are likely explained by our inability to experimentally control the velocity at which our participants performed plantar flexion contractions. In our study, rate of torque development increased with contraction level (Supplemental Fig. S1). This "velocity" effect on gearing is similar to a previous in vivo study that also observed an increase in gearing with velocity (20) and aligns with the findings of Azizi et al. (2) that high-velocity contractions are associated with high gearing, although in our case force was also high. High gearing at high-force/high-velocity contractions may be mechanically beneficial as it allows muscle fibers to shorten at slower velocities than the whole muscle,

Downloaded from journals.physiology.org/journal/jappl (078.056.041.167) on November 9, 2026.

thereby optimizing force production. Our results also demonstrate that in some participants, gearing values were as low as 0.8, specifically in the LG of older adults at very low contraction levels (Fig. 2*C*). Previous studies report gearing values typically >1 in pennate muscles and suggest that gearing is 1 in contractions whereby pennation angle does not change and thickness decreases (3). Here, we show that not only does the LG get thinner during low-force contraction (10% MVC) but also that pennation angle decreases during the contraction, particularly in older adults (Fig. 2, *A* and *B*). This may be linked to the interaction between the bulging and deformation of surrounding muscles, which have been shown to possess different activation profiles (33), although this requires further exploration. Furthermore, we did not see a common pattern of muscle bulging in thickness with increased fiber rotation and gearing as described in previous work (2). Rather, we found that the MG shortened and rotated more than the LG at maximal contraction levels but had minimal increases in thickness. To remain isovolumetric, increased fiber shortening must be accompanied by changes in muscle girth. The small increases in thickness, and in some participants even decreases in muscle thickness, suggest that the MG bulged more than the LG in the width direction, as observed in previous animal studies (34). Thus, it could be that muscle gearing is determined not only by how much a muscle is able to bulge in thickness but also by how much it is able to bulge in either direction, in this case width, to remain in constant volume during muscle shortening. Future studies using imaging to measure transverse muscle deformations (35) are necessary to examine this possibility.

In this study, shear modulus was not different between our young and older adults, however, it was greater in the MG compared with the LG. Muscles with higher shear modulus demonstrated smaller changes in thickness at maximal contraction levels, with no relationship between shear modulus and gearing. These results differ from those previously demonstrated in aging rats, whereby increases in connective tissue stiffness were associated with higher gearing (4). These differences could be attributed to the less variation in muscle properties between young and older participants across studies. Across our population, muscle shear modulus varied from 8.2 to 9.2 kPa in the MG of our young and older humans, whereas fiber bundle modulus was 19.1 and 39.1 kPa in young and older rats, respectively. Furthermore, we used shear wave elastography to measure shear modulus in vivo, whereas Holt et al. (4) used traditional mechanical tests to assess muscle properties in vitro. It should also be noted that much of the work on muscle shape change and gearing has examined isolated muscle during supramaximal contractions, which does not account for a muscle's interaction with surrounding muscles, bones, or connective tissues. Both animal and human experiments have demonstrated that altering a muscle's ability to deform influences its mechanical behavior. For example, when polypropylene sleeves are used to physically constrain a muscle's bulging, both muscle shortening and work output decrease (9). de Brito Fontana et al. (36) demonstrated that the quadriceps produce less force when activated together when compared with the sum of their individual forces if each muscle was activated in isolation. When the human MG is transversely loaded during contractions, both bulging and fiber rotation decrease (37). Future studies that capture the synchronous shape changes of synergist muscles during contractions, for example, how the underlying soleus interacts with the gastrocnemii, will allow for a better understanding of the functional implications of muscle deformation.

Here, we show that muscles with greater amounts of intramuscular fat undergo smaller changes in pennation angle—but only during high-force isometric contractions. An exploratory analysis, whereby we torque-matched a subset of our nine young and nine older adults who demonstrated maximum isometric torque within 5 Nm, demonstrated this relationship was no longer present. Therefore, this finding is likely explained by older adults with lower strength having less absolute fiber rotation during maximal contractions and higher levels of intramuscular fat. Fat content was similar between the LG, MG, and SOL in the young group, however in the older group, the MG and SOL had greater amounts of intramuscular fat than the LG. This is evident in Fig. 3*C*, with the MG of older adults (solid red circles) extending this relationship in the negative direction. Intramuscular fat may affect muscle fiber dynamics by limiting fiber shortening and bulging, subsequently causing less fiber rotation. Gearing was lower in older adults across all contraction levels, and although this was not related to intramuscular fat, it may be due to the age-related strength deficit. An increase in intramuscular fat content results in less contractile components and ultimately lower force generated by the muscle (17). This is confirmed by our older adults having significantly lower maximal torque compared with that of our young adults, paired with higher fat content.

Muscles with greater fat-corrected PCSA have more fiber rotation and higher gearing during both submaximal and maximal contraction levels. Muscle thickness, however, appeared to vary across contraction levels. At 100% MVC, muscles with higher PCSA got thinner, whereas muscles with lower PCSA got thicker. We can see where the MG and LG fall along this relationship in Fig. 3*D*, with the LG (blue) at the lower end of fat-corrected PCSA but bulging in thickness the most and the MG (red) at the higher end of fat-corrected PCSA and getting thinner. However, at 30% MVC, the trend reverses and fat-corrected PCSA is positively related to a muscle bulging in thickness (Fig. 4*D*). The MG has a greater force-generating capacity than the LG, and thus may be able to exceed the internal resistance of passive tissues within the muscle (i.e., intramuscular fat and connective tissue) to accommodate shortening by increasing width at higher contraction levels. Intriguingly, the MG is stiffer than the LG, and thus the higher forces must be sufficient to overcome the greater resistance to muscle bulging. A greater number of fibers in parallel would create a greater force to pull the aponeurosis together, however, the muscle would have greater fiber shortening and radial bulging, thus the muscle undergoes increased fiber rotation and higher gearing without significant increases in thickness, as seen in the muscle shape change and gearing patterns of the MG. Pennate muscles compress less in thickness during low-force contractions owing to a smaller fiber force pulling the aponeurosis together. At higher forces, this increased thickness force leads to increased forces in the radial direction that can no longer be resisted by connective tissues, causing the muscle to deform in the width direction. Thus, the different

Downloaded from journals.physiology.org/journal/jappl (078.056.041.167) on November 9, 2026.

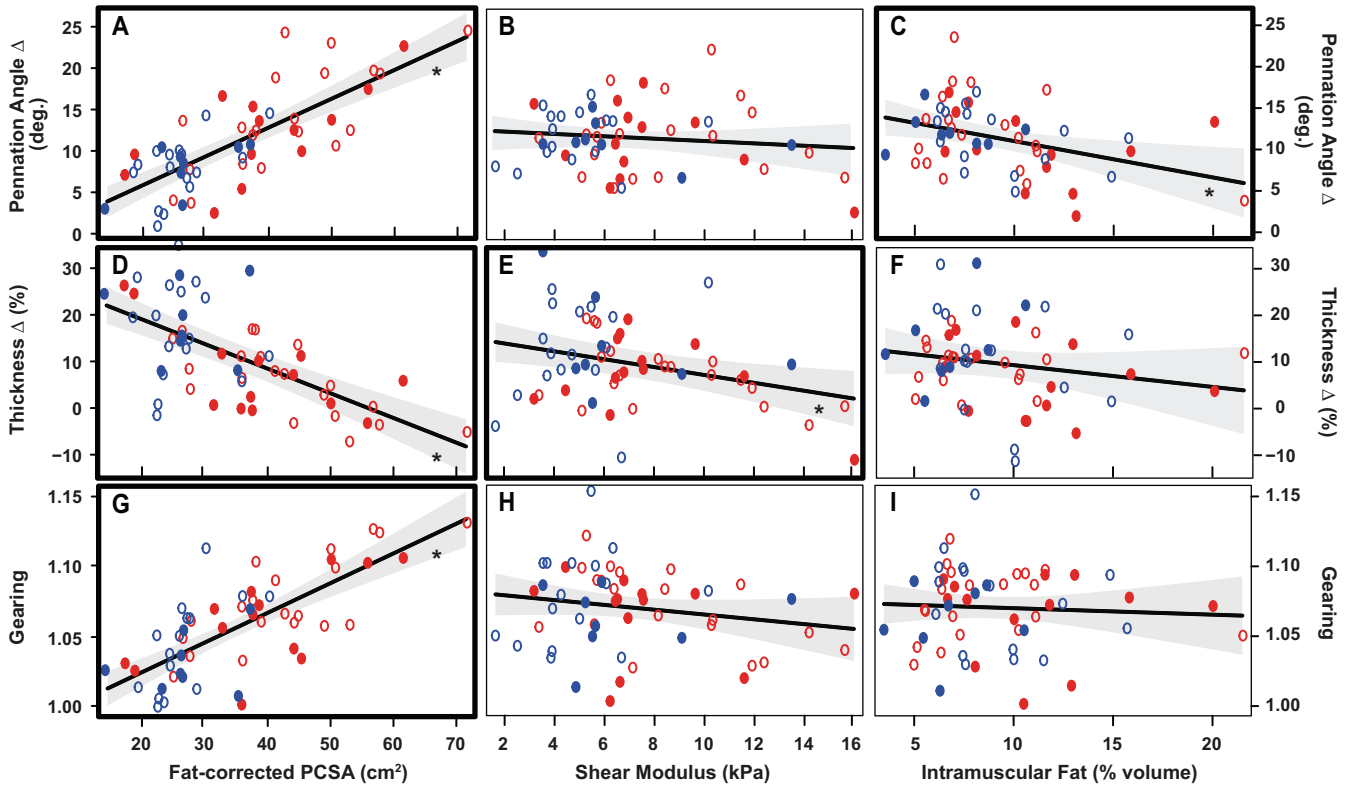


Figure 3. Influence of internal muscle properties on muscle shape change and gearing at 100% MVC. Predictor effect plots based on the linear mixed-effects models. Plots display the relationship between fat-corrected physiological cross-sectional area (PCSA), shear modulus, and intramuscular fat and the change in pennation angle (*A*, *B*, *C*, respectively), as well as the change in muscle thickness (*D*, *E*, *F*, respectively) and gearing (*G*, *H*, *I*, respectively). The black lines indicate the partial slope of predictors to the response, when other predictors are held fixed. The gray-shaded area indicates a pointwise confidence band of the fitted values, based on standard errors computed from the covariance matrix of the fitted regression coefficients (38). Partial residual points are displayed to showcase where other factors such as age, older (●) and young (○), and muscle; medial gastrocnemius (red) and lateral gastrocnemius (blue) fit along the slope. *Darker lined boxes indicates significant effect of predictor on the response. MVC, maximal voluntary contraction.

relationship between fat-corrected PCSA and bulging at low and high contraction levels is likely due to the transition point in the resistive capacity of the connective tissue. Previous studies have shown that increases in connective tissue resistance (4) and disruptions to the integrity of the aponeurosis (11) both influence gearing only during high-force contractions—which together with our results suggests an intensity-dependent effect of internal muscle properties on shape changes and gearing. Another factor that must be considered, and is often overlooked, is that the muscles within the triceps surae are packaged within a synergistic muscle compartment, which means that individual muscle deformations would likely affect the behavior of the surrounding muscles. Synergistic muscles with greater PCSA have been shown to be preferentially activated during submaximal contractions (33), therefore the relative timing of activation (and thus deformation) may also influence the interaction between muscles and accompany dynamic shape changes, although this requires further investigation.

Of note, when assessing the influence of internal muscle properties on shape change and gearing, we did not include age or muscle as factors (Figs. 3 and 4), despite the observed muscle and age effect on muscle properties (Table 3) and dynamic shape changes (Fig. 2). This was done to extend the variability within our dataset and create a greater spectrum of muscle properties. Additional analyses, whereby the influence of internal muscle properties on shape change and gearing was identified for each individual muscle and included the age effect, displayed similar results; the only difference being the relationship between muscle thickness and fat-corrected PCSA, which can be explained by the opposing bulging behavior of the MG and LG. In this case, it is challenging to determine whether the negative relationship between muscle thickness and fat-corrected PCSA that we observed is due to unique differences between these two muscles or would persist if additional muscles with varying internal muscle properties were included in the analysis. Nonetheless, future studies that integrate comprehensive in vivo measures across multiple muscles would yield further insights.

In this study, we used multimodal imaging to explore how internal muscle properties including muscle shear modulus, intramuscular fat, and fat-corrected PCSA modulate muscle shape change and gearing in vivo. Our results highlight that a muscle's force-generating capacity, indicated by its fat-corrected PCSA, may play a dominant role in fiber rotation, bulging, and gearing—particularly during high-force contractions. In addition, we found that muscle stiffness and intramuscular fat both influence muscle dynamics, with higher shear modulus and fat content associated with limited muscle bulging

Downloaded from journals.physiology.org/journal/jappl (078.056.041.167) on November 9, 2026.

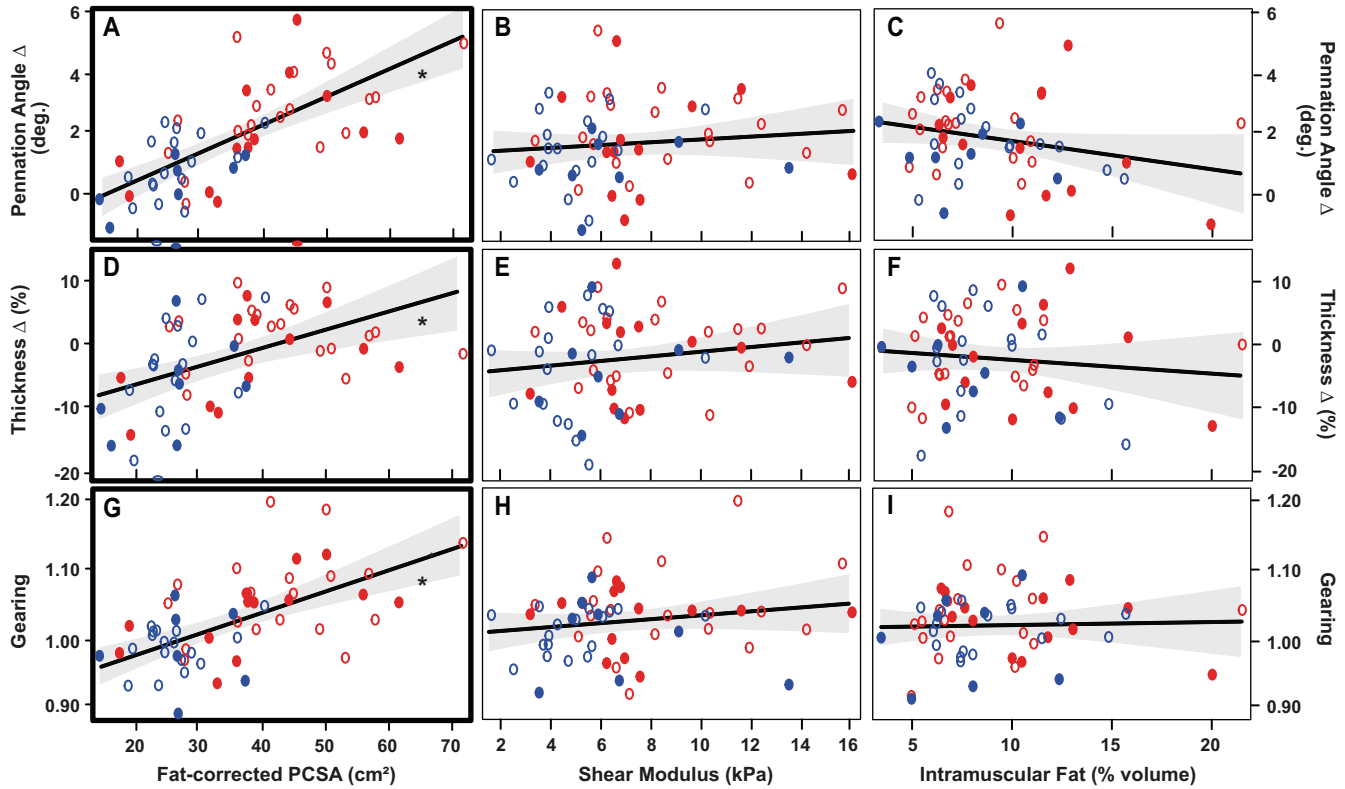


Figure 4. Influence of internal muscle properties on muscle shape change and gearing at 30% MVC. Predictor effect plots based on the linear mixed-effects models. Plots display the relationship between fat-corrected physiological cross-sectional area (PCSA), shear modulus, and intramuscular fat and the change in pennation angle (*A*, *B*, *C*, respectively), as well as the change in muscle thickness (*D*, *E*, *F*, respectively) and gearing (*G*, *H*, *I*, respectively). The black lines indicate the partial slope of predictors to the response, when other predictors are held fixed. The gray-shaded area indicates a pointwise confidence band of the fitted values, based on standard errors computed from the covariance matrix of the fitted regression coefficients (38). Partial residual points are displayed to showcase where other factors such as age, older (●) and young (○), and muscle; medial gastrocnemius (red) and lateral gastrocnemius (blue) fit along the slope. *Darker lined boxes indicates significant effect of predictor on the response. MVC, maximal voluntary contraction.

and fiber rotation, respectively. These findings support the hypothesis that variable changes in muscle shape and gearing result from the interaction between contractile forces and internal muscle properties (4, 11), and also suggest that submaximally activated muscles behave differently in vivo than isolated muscles, contracting maximally at constant lengths or loads. This is, in part, supported by experimental evidence that the removal of a muscle from its compartment within a limb influences its force output (39) and that force-length relationships differ between submaximally and maximally activated muscles (40, 41). An improved understanding of how internal muscle properties influence a muscle's mechanical response to force has implications for preventing and treating muscle deficits associated with aging, disease, and disuse. Future investigations into the interactions between synergistic muscles within a compartment and how their dynamic changes in activation and fascicle behavior influence 3-D deformations among neighboring muscles will provide further insights into the mediators of muscle shape change and gearing.

DATA AVAILABILITY

Data can be found at http://doi.org/10.6084/m9.figshare.23164502.

SUPPLEMENTAL DATA

Supplemental Tables S1 and S2 and Supplemental Fig. S1: http://doi.org/10.6084/m9.figshare.22059575.

ACKNOWLEDGMENTS

We acknowledge the University of Queensland (UQ) Centre for Advanced Imaging for the assistance with MRI and Romain Feigean and India Lindemann for the support in data collection and processing.

DISCLOSURES

No conflicts of interest, financial or otherwise, are declared by the authors.

AUTHOR CONTRIBUTIONS

N.Y.K. and T.J.M.D. conceived and designed research; N.Y.K. and S.P. performed experiments; N.Y.K., C.J.C., F.H., and S.P. analyzed data; N.Y.K., K.T., F.H., and T.J.M.D. interpreted results of experiments; N.Y.K. prepared figures; N.Y.K. drafted manuscript; N.Y.K., C.J.C., K.T., F.H., and T.J.M.D. edited and revised manuscript; N.Y.K., C.J.C., K.T., F.H., S.P., and T.J.M.D. approved final version of manuscript.

Downloaded from journals.physiology.org/journal/jappl (078.056.041.167) on November 9, 2026.

REFERENCES

1. **Baskin RJ**, **Paolini PJ.** Volume change and pressure development in muscle during contraction. *Am J Physiol* 213: 1025–1030, 1967. doi:10.1152/ajplegacy.1967.213.4.1025.
2. **Azizi E**, **Brainerd EL**, **Roberts TJ.** Variable gearing in pennate muscles. *Proc Natl Acad Sci USA* 105: 1745–1750, 2008. doi:10.1073/pnas.0709212105.
3. **Brainerd EL**, **Azizi E.** Muscle fiber angle, segment bulging and architectural gear ratio in segmented musculature. *J Exp Biol* 208: 3249–3261, 2005. doi:10.1242/jeb.01770.
4. **Holt NC**, **Danos N**, **Roberts TJ**, **Azizi E.** Stuck in gear: age-related loss of variable gearing in skeletal muscle. *J Exp Biol* 219: 998–1003, 2016. doi:10.1242/jeb.133009.
5. **Dick TJM**, **Wakeling JM.** Geometric models to explore mechanisms of dynamic shape change in skeletal muscle. *R Soc Open Sci* 5: 172371, 2018. doi:10.1098/rsos.172371.
6. **Dick TJM**, **Wakeling JM.** Shifting gears: dynamic muscle shape changes and force-velocity behavior in the medial gastrocnemius. *J Appl Physiol (1985)* 123: 1433–1442, 2017. doi:10.1152/japplphysiol.01050.2016.
7. **Son J**, **Rymer WZ.** Loss of variable fascicle gearing during voluntary isometric contractions of paretic medial gastrocnemius muscles in male chronic stroke survivors. *J Physiol* 598: 5183–5194, 2020. doi:10.1113/JP280126.
8. **Kelp NY**, **Gore A**, **Clemente CJ**, **Tucker K**, **Hug F**, **Dick TJM.** Muscle architecture and shape changes in the gastrocnemii of active younger and older adults. *J Biomech* 129: 110823, 2021. doi:10.1016/j.jbiomech.2021.110823.
9. **Azizi E**, **Deslauriers AR**, **Holt NC**, **Eaton CE.** Resistance to radial expansion limits muscle strain and work. *Biomech Model Mechanobiol* 16: 1633–1643, 2017. doi:10.1007/s10237-017-0909-3.
10. **Sleboda DA**, **Roberts TJ.** Incompressible fluid plays a mechanical role in the development of passive muscle tension. *Biol Lett* 13: 20160630, 2017. doi:10.1098/rsbl.2016.0630.
11. **Eng CM**, **Azizi E**, **Roberts TJ.** Structural determinants of muscle gearing during dynamic contractions. *Integr Comp Biol* 58: 207–218, 2018. doi:10.1093/icb/icy054.
12. **Roberts TJ**, **Eng CM**, **Sleboda DA**, **Holt NC**, **Brainerd EL**, **Stover KK**, **Marsh RL**, **Azizi E.** The multi-scale, three-dimensional nature of skeletal muscle contraction. *Physiology (Bethesda)* 34: 402–408, 2019. doi:10.1152/physiol.00023.2019.
13. **Biltz NK**, **Collins KH**, **Shen KC**, **Schwartz K**, **Harris CA**, **Meyer GA.** Infiltration of intramuscular adipose tissue impairs skeletal muscle contraction. *J Physiol* 598: 2669–2683, 2020. doi:10.1113/JP279595.
14. **Pinel S**, **Kelp NY**, **Bugeja JM**, **Bolsterlee B**, **Hug F**, **Dick TJM.** Quantity versus quality: age-related differences in muscle volume, intramuscular fat, and mechanical properties in the triceps surae. *Exp Gerontol* 156: 111594, 2021. doi:10.1016/j.exger.2021.111594.
15. **Goodpaster BH**, **Chomentowski P**, **Ward BK**, **Rossi A**, **Glynn NW**, **Delmonico MJ**, **Kritchevsky SB**, **Pahor M**, **Newman AB.** Effects of physical activity on strength and skeletal muscle fat infiltration in older adults: a randomized controlled trial. *J Appl Physiol (1985)* 105: 1498–1503, 2008. doi:10.1152/japplphysiol.90425.2008.
16. **Therkelsen KE**, **Pedley A**, **Speliotes EK**, **Massaro JM**, **Murabito J**, **Hoffmann U**, **Fox CS.** Intramuscular fat and associations with metabolic risk factors in the Framingham Heart Study. *Arterioscler Thromb Vasc Biol* 33: 863–870, 2013. doi:10.1161/ATVBAHA.112.301009.
17. **Rahemi H**, **Nigam N**, **Wakeling JM.** The effect of intramuscular fat on skeletal muscle mechanics: implications for the elderly and obese. *J R Soc Interface* 12: 20150365, 2015. doi:10.1098/rsif.2015.0365.
18. **Powell PL**, **Roy RR**, **Kanim P**, **Bello MA**, **Edgerton VR.** Predictability of skeletal muscle tension from architectural determinations in guinea pig hindlimbs. *J Appl Physiol Respir Environ Exerc Physiol* 57: 1715–1721, 1984. doi:10.1152/jappl.1984.57.6.1715.
19. **Dick TJ**, **Hug F.** Advances in imaging for assessing the design and mechanics of skeletal muscle in vivo. *J Biomech* 155: 111640, 2023. doi:10.1016/j.jbiomech.2023.111640.
20. **Randhawa A**, **Jackman ME**, **Wakeling JM.** Muscle gearing during isotonic and isokinetic movements in the ankle plantarflexors. *Eur J Appl Physiol* 113: 437–447, 2013. doi:10.1007/s00421-012-2448-z.
21. **Dixon WT.** Simple proton spectroscopic imaging. *Radiology* 153: 189–194, 1984. doi:10.1148/radiology.153.1.6089263.
22. **Gennisson JL**, **Deffieux T**, **Fink M**, **Tanter M.** Ultrasound elastography: principles and techniques. *Diagn Interv Imaging* 94: 487–495, 2013. doi:10.1016/j.diii.2013.01.022.
23. **Le Sant G**, **Nordez A**, **Andrade R**, **Hug F**, **Freitas S**, **Gross R.** Stiffness mapping of lower leg muscles during passive dorsiflexion. *J Anat* 230: 639–650, 2017. doi:10.1111/joa.12589.
24. **Eby SF**, **Song P**, **Chen S**, **Chen Q**, **Greenleaf JF**, **An KN.** Validation of shear wave elastography in skeletal muscle. *J Biomech* 46: 2381–2387, 2013. doi:10.1016/j.jbiomech.2013.07.033.
25. **Cronin NJ**, **Carty CP**, **Barrett RS**, **Lichtwark G.** Automatic tracking of medial gastrocnemius fascicle length during human locomotion. *J Appl Physiol (1985)* 111: 1491–1496, 2011. doi:10.1152/japplphysiol.00530.2011.
26. **Pinheiro JC**, **Bates DM**, **DebRoy SS**, **Sarkar D.** NIme: linear and nonlinear mixed effects models. *R package version 31-110* 3: 1–113, 2013.
27. **Hothorn T**, **Bretz F**, **Westfall P.** Simultaneous inference in general parametric models. *Biom J* 50: 346–363, 2008. doi:10.1002/bimj.200810425.
28. **Hamard R**, **Aeles J**, **Kelp NY**, **Feigean R**, **Hug F**, **Dick TJM.** Does different activation between the medial and the lateral gastrocnemius during walking translate into different fascicle behavior? *J Exp Biol* 224: jeb242626, 2021. doi:10.1242/jeb.242626.
29. **Maganaris CN**, **Baltzopoulos V**, **Sargeant AJ.** In vivo measurements of the triceps surae complex architecture in man: implications for muscle function. *J Physiol* 512: 603–614, 1998. doi:10.1111/j.1469-7793.1998.603be.x.
30. **Wakeling JM**, **Blake OM**, **Wong I**, **Rana M**, **Lee SS.** Movement mechanics as a determinate of muscle structure, recruitment and coordination. *Philos Trans R Soc Lond B Biol Sci* 366: 1554–1564, 2011. doi:10.1098/rstb.2010.0294.
31. **Narici MV**, **Binzoni T**, **Hiltbrand E**, **Fasel J**, **Terrier F**, **Cerretelli P.** In vivo human gastrocnemius architecture with changing joint angle at rest and during graded isometric contraction. *J Physiol* 496: 287–297, 1996. doi:10.1113/jphysiol.1996.sp021685.
32. **Azizi E**, **Roberts TJ.** Geared up to stretch: pennate muscle behavior during active lengthening. *J Exp Biol* 217: 376–381, 2014. doi:10.1242/jeb.094383.
33. **Crouzier M**, **Lacourpaille L**, **Nordez A**, **Tucker K**, **Hug F.** Neuromechanical coupling within the human triceps surae and its consequence on individual force-sharing strategies. *J Exp Biol* 221: jeb187260, 2018. doi:10.1242/jeb.187260.
34. **Konow N**, **Collias A**, **Biewener AA.** Skeletal muscle shape change in relation to varying force requirements across locomotor conditions. *Front Physiol* 11: 143, 2020. doi:10.3389/fphys.2020.00143.
35. **Randhawa A**, **Wakeling JM.** Transverse anisotropy in the deformation of the muscle during dynamic contractions. *J Exp Biol* 221: jeb175794, 2018. doi:10.1242/jeb.175794.
36. **de Brito Fontana H**, **de Campos D**, **Sawatsky A**, **Han SW**, **Herzog W.** Why do muscles lose torque potential when activated within their agonistic group? *J Exp Biol* 223: jeb213843, 2020. doi:10.1242/jeb.213843.
37. **Ryan DS**, **Stutzig N**, **Siebert T**, **Wakeling JM.** Passive and dynamic muscle architecture during transverse loading for gastrocnemius medialis in man. *J Biomech* 86: 160–166, 2019. doi:10.1016/j.jbiomech.2019.01.054.
38. **Fox J**, **Weisberg S.** Visualizing fit and lack of fit in complex regression models with predictor effect plots and partial residuals. *J Stat Soft* 87: 1–27, 2018. doi:10.18637/jss.v087.i09.
39. **Ruttiman RJ**, **Sleboda DA**, **Roberts TJ.** Release of fascial compartment boundaries reduces muscle force output. *J Appl Physiol (1985)* 126: 593–598, 2019. doi:10.1152/japplphysiol.00330.2018.
40. **Holt NC**, **Azizi E.** What drives activation-dependent shifts in the force–length curve? *Biol Lett* 10: 20140651, 2014. doi:10.1098/rsbl.2014.0651.
41. **de Brito Fontana H**, **Herzog W.** Vastus lateralis maximum force-generating potential occurs at optimal fascicle length regardless of activation level. *Eur J Appl Physiol* 116: 1267–1277, 2016. doi:10.1007/s00421-016-3381-3.

Downloaded from journals.physiology.org/journal/jappl (078.056.041.167) on November 9, 2026.